Bull. Mater. Sci., Vol. , No. , , pp. 1–9 © Indian Academy of Sciences
DOI XX.XXXX/XXXXXX-XXX-XXX-X

Predictive Modeling of Hardness Values and Phase Fraction Percentages in Micro-Alloyed Steel During Heat Treatment Using AI

ANKUR BASSI*, SOHAM BODAS, SHUJA HASAN and SESHASAI SRINIVASAN

wbooth school of engineering, McMaster University

MS received ; accepted

Abstract. In this work, we have proposed a predictive model that can determine the hardness and phase fraction percentages of micro-alloyed steel with a predefined chemical composition during heat treatment under specific cooling conditions. The model uses a feed-forward neural network enhanced by the ensemble method. The model has been trained on experimental data derived from Continuous Cooling Transformation (CCT) diagrams for 39 unique steel types. The inputs to the model include a cooling profile defined by a set of time-temperature values, and the chemical composition of the steel. Sensitivity analysis was performed using the validated model to understand the impact of key input variables, including individual alloys and process steps. This analysis, which measures the variability in output in response to changes in a specific input variable, showed a significant correlation with experimental findings and literature reports. Thus, our model not only predicts steel properties under varied cooling conditions but also aligns with existing theoretical knowledge and experimental data.

Keywords. Multiphase steels; Thermomechanical processing; neural network model; mechanical properties; continuous cooling transformation

1. Introduction

Steel manufacturing entails the meticulous selection and proportioning of materials to yield the desired steel properties. The process involves heating the steel to a high temperature, followed by a controlled cooling phase – a process known as Continuous Cooling Transformation (CCT). This method is instrumental in bestowing steel with its characteristic properties.

Steel's ubiquitous application worldwide necessitates variants with specific properties such as hardness, ductility, and tensile strength. These attributes are governed by the phase fractions within the steel's micro structure[1,2,3] . This micro structure is determined by a combination of factors, including the steel's chemical composition and the manufacturing processes employed[4–6] . Thus, the ability to predict these properties based on the steel's microstructure has become an area of intensive research, intending to enhance the performance of steel in various applications.

Earlier studies have focused on the relationship between mechanical properties and the microstructure of steel, offering significant insights into the role of dislocation density, lath thickness, alloying elements, and volume fractions of secondary particles[4] . However, predicting these properties remains a complex challenge due to the numerous variables[4], from alloying elements to rolling and cooling conditions.

* Author for correspondence (bassia8@mcmaster.ca)

In light of previous research[7–11] showing the effectiveness and suitability of neural network models for such challenges, this study aims to develop a neural network model capable of predicting microstructural phase fractions and hardness values of steel, based on its composition and heat treatment profiles. Specifically, our focus lies in identifying the optimal Continuous Cooling Transformations that yield the desired mechanical properties of the steel.

This research has three primary objectives:

1. To curate a comprehensive steel database from the CCT diagrams in the steel atlas[12] . This database will encompass temperature, time, phase fractions, and hardness values.

2. To develop a neural network model capable of predicting steel hardness values and microstructure volume fractions, given its composition and continuous cooling transformation profile.

3. To conduct sensitivity analysis on the model to understand the impact of key input variables on the predicted output, providing further insight into the relationships between steel composition, heat treatment processes, and resulting properties.

2. Literature Review

The study by C.-C Huang, Y.-T Chen, Y.-J Chen, C.-Y Chang, H.-C Huang, R.-C Hwang effectively utilized 1400

data sets, which included billet compositions, control parameters of the rolling process, and mechanical properties of the rolled steel bars as inputs to the neural network. The AI analyzer confidently predicted critical factors such as yield strength, tensile strength, and elongation percentage for the rolled steel bars. This new technology can precisely set related control parameters on the bar rolling process to enhance the quality of steel bars while simultaneously reducing production costs[7].

According to a research paper by H Monajati, D Asefi, A Parsapour, Abbasi, Sh the authors used an artificial neural network (ANN) to analyze how processing parameters affect the formability of deep drawing quality (DDQ) steel sheets. To accurately model mechanical and formability properties, such as yield strength, work hardening exponent, and anisotropy, a detailed description of the material's chemical composition was necessary. This resulted in the use of 19 input variables to analyze the properties. The optimal results were achieved using two hidden layers with 19 neurons each.

After constructing the model, the researchers investigated the influence of various parameters on the formability of carbon steel. For instance, they examined the effect of carbon content by keeping all other parameters constant while varying the carbon content from 0.0032 to 0.062[8].

The researchers also analyzed the effects of finishing and coiling temperatures (FT and CT) on the steel's properties. To do this, they used all parameters except for FT and CT, which were varied from 854 to 910 and 540 to 625 C, respectively. Finally, the effects of heating rate and soaking time were examined by varying these parameters.

In another study Z Sterjovski, D Nolan, K R Carpenter, D P Dunne, J Norrish(2005) , evaluated the effectiveness of three back-propagation artificial neural network models in predicting various mechanical properties of steel. These included the impact toughness of quenched and tempered pressure vessel steel exposed to multiple post weld heat treatment cycles, the hardness of the simulated heat affected zone in pipeline and tap fitting steels after in-service welding, and the hot ductility and hot strength of various micro alloyed steels in the continuous casting process. The ANNs proved to be successful in predicting these properties, as demonstrated by the close match between predicted and actual experimental values. The authors utilized 150,000-500,000 cycles/iterations to minimize and stabilize the RMS error. The study also examined four micro-alloyed steels (Nb, Nb-Ti, Ti, and C-Mn-Al) of various chemical compositions, with tensile test specimens that were cylindrical in shape with a 10mm diameter and a gauge length of 95mm[9].

G Sidhu, S D Bhole, D L Chen, E Essadiqi(2011) employed artificial neural network to accurately determine the volume fraction of bainite in low carbon steels. The dataset, which comprised of 437 data points, was analyzed through rigorous comparison of 25 network performances. The neural network's input included vital information such as chemical composition (C, Si, Mo, Cr, V, Ni, Mn), the highest temperature of bainite formation, the isothermal transformation temperature, and the transformation time. Additionally, the study delved into analyzing the impact of alloying element composition on bainite volume fraction, and the results obtained were in line with established metallurgical theory. This study has successfully demonstrated the capability of artificial neural networks in accurately predicting bainite volume fraction, thereby paving the way for further advancements in the field of metallurgy[10].

In the study by G Sidhu, S D Bhole, D L Chen, E Essadiqi, a training was executed on a dataset consisting of 175 data points until it met one of the predetermined termination criteria. These criteria included:

(i) the achievement of 100,000 iterations,

(ii) a reduction in the mean square error of the network to less than 0.001, or

(iii) the gradient of the search direction in the Levenberg-Marquardt Backpropagation (LMBP) algorithm falling below 1 x 10-9.

To predict hardness, the study considered not only the chemical composition but also the heat treatment conditions, specifically the austenitization temperature (Taus), isothermal transformation time (tiso), and isothermal transformation temperature (Tiso). The network's performance was evaluated by applying the remaining 47 data points from the database, which were not included in the initial training. Furthermore, the model was utilized to predict the hardness of five newly designed bainitic steels[11].

In the study by S Srinivasan , we see that finding the optimal alloying elements using AI with particle swarm algorithm for a fast global search on a multi-dimensional search space to obtain steels with a specific hardness value.

$$F = \left|\frac{HV - HV_{\text{target}}}{HV_{\text{target}}}\right| + \left|\frac{C}{c_{\text{target}}}\right|$$

Here the cost is minimized with the PSO algorithm. The PSO uses hardness value and C is calculated from the reduced-order hardness model[13].

X Huang, H Wang, W Xue, S Xiang, H Huang, L Meng, G Ma, A Ullah, G Zhang (2020) , TTT diagrams are used to study the microstructure of stainless steel, and the importance of TTT diagrams is discussed[14]. Hence, to accurately extract the information from such diagrams, different ML (Machine Learning) algorithms have been used and compared to check the accuracy. Algorithms including BP artificial neural network, Random Committee, Random Forest, and Bagging, are developed for prediction of TTT diagram with relevant descriptors containing the alloying elements, austenitizing temperature and holding time. The results show that such combinations can achieve high predictive accuracy on the TTT diagrams of stainless steel with a high correlation coefficient value and low root mean squared error value.

Moreover, in the research by X Geng, H Wang, W Xue, S Xiang, H Huang, L Meng, G Ma(2020) , CCT diagrams are used for extracting data and discussing why they are important[15]. In this study, machine learning approaches are provided to predict CCT diagrams of tool steels using rel-

evant material descriptors including the chemical compositions, austenitizing temperature and cooling rate. Random forest is proved to be the best model to predict pearlite transition temperature and martensite transformation start temperature accurately. K-Nearest Neighbours and Bagging are suitable for predicting the start and end temperatures of bainite formation, respectively. These optimal models are then used to predict the CCT diagrams of T8, 6CrW2Si, 4CrMoV, CrMn and Cr12W.

3. Methods

3.1 *Database Creation*

The Continuous Cooling Transformation (CCT) diagram is a crucial tool in describing the continuous cooling process of steel, displaying temperature versus time and providing distinct cooling profiles for each steel type, resulting in unique microstructures and hardness values. Figure 2 serves as an excellent example of this. The CCT diagram contains significant information such as chemical composition, cooling profiles, hardness values, and the percentage of each microstructure produced by each cooling profile.

To conduct this study, we extracted data[16] points from multiple CCT diagrams (as shown in Figure 1) sourced from various types of steel documented in the steel atlas[12] . The dataset consists of 38 columns, including time-temperature pairs, chemical compositions, phase fractions, and hardness values, which is the target column. In total, the dataset includes 380 records derived from 39 distinct steel types.

To address the limited size of the dataset and potential experimental variability (with errors of approximately ±0.2%), we implemented a data augmentation strategy. This approach adjusted hardness values by ±0.2% while keeping other input parameters constant. By doing so, we aimed to expand the dataset and balance the need for a larger dataset against the constraints of data availability and experimental variability. We then shuffled the augmented dataset and retained eighty percent as training data and used the remaining twenty percent for testing.

3.2 *Formulating Cooling Profile Equation for input*

Initially in the project, to provide time temperature pairs of a single cooling profile as an input to NN, it was decided to transform these pairs into a line equation that would make sense to the NN to understand it as a single line. The two ways implemented were Lagrange's Interpolation[17] and Least Square approximation[18;19] . Once the equation was formed, the coefficients of the equation were used as input parameters representing the cooling profiles instead of the temperature-time pairs. It was noted that equations with degree three were enough to represent all the cooling profiles in the entire data set. Hence, all the temperature-time pairs were converted into 3^{rd} degree equation and used as coefficients along with composition of steels inputs for model training. Table 1 below shows the results of the Mean Relative Error MRE obtained after transforming the data using the two mentioned methods and feeding the inputs to the NN model for training and testing. When comparing the MRE from both the methods it seems that Least Square Approximation gives better results as seen in table below.

Table 1. Input Parameters Range

Input Parameter	Range
C(wt%)	0.1 – 2.19
Si(wt%)	0 – 1.05
Ni(wt%)	0 – 3.03
Mn (wt%)	0.2 – 1.98
Mo (wt%)	0 – 0.56
Cr (wt%)	0 – 13.12
V (wt%)	0 – 0.31
Cu (wt%)	0 – 0.91
Al (wt%)	0 – 0.063
N (wt%)	0 – 0.003
P (wt%)	0 – 0.44
S (wt%)	0 – 0.29
B (wt%)	0 – 0.05
W (wt%)	0 – 1.15
Ti (wt%)	0 – 0 .18
T (C)	140.48 – 1774.62
t (s)	0.100122-188000

Table 2. Distribution of output parameters

Output	Range
HV	90-960
Austenite	0-30
Ferrite	0-92
Pearlite	0-100
Bainite	0-100
Martensite	0-99

3.3 *Providing Time-temperature pair as input*

Later, during investigation, it was found that the time-temperature pairs, if provided directly to the NN model, it provide much better R^2 as compared to the coefficient inputs obtained from the Least Square Approximation method. As a result, the final architecture included time-temperature values along with the chemical compositions of steel for training the model to predict the hardness of steel.

Table 3. MRE Comparison

	Lagrange Interpolation MRE	Least Square Approximation MRE
Mode	82.0975	12.9347
Mean	5.6517	2.26397
Median	2.7776	1.4660

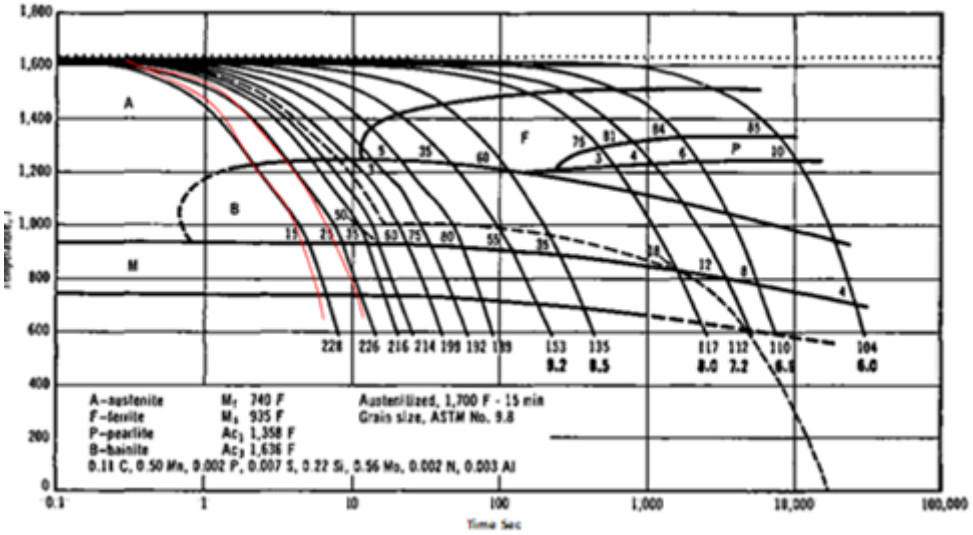

Figure 1. Red Lines highlight first 2 Cooling Profiles obtained from steel atlas [12]

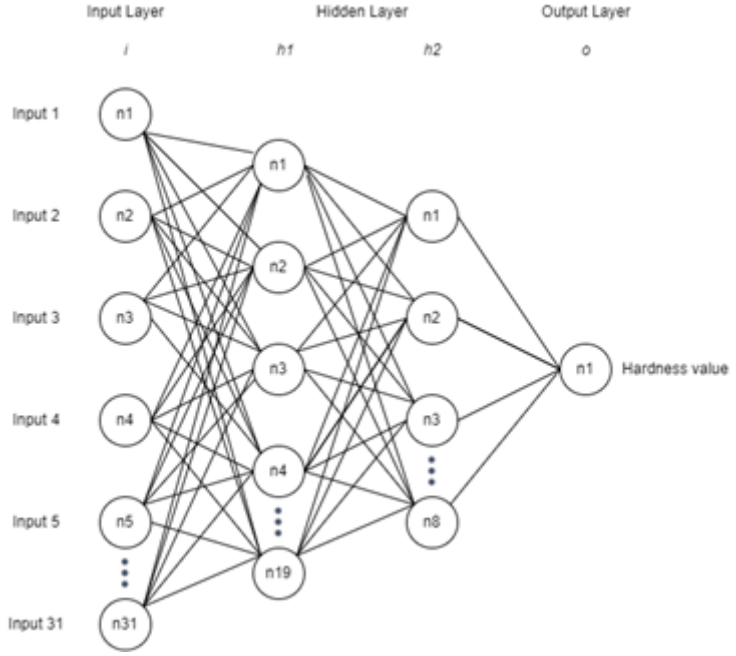

Figure 2. Neural Network Architecture

3.4 *Neural Network Architecture for Hardness*

In this research, a three-layer neural network known as a Multilayer Perceptron (MLP), a type of feedforward neural network, was employed. The MLP was chosen for its capacity to manage multiple inputs, model non-linear relationships, and flexibility regarding architectural modifications. It was well-suited for predicting steel hardness based on a dataset consisting of 23 features.

The third layer of the network, the output layer, incorporated a single neuron, its output correlating with the hardness value of the steel for a specific heat treatment condition. The number of neurons (nH) in the first and second layers, which serve as the hidden layers, were determined following an exhaustive investigation that involved testing various combinations of hyper-parameters for the neural network to achieve the best R2 value.

The need for this rigorous exploration stems from the fact that the number of neurons in these hidden layers significantly impacts both the accuracy and complexity of the neural network[20] . Too few neurons may inadequately capture the trend of the training database, while too many neurons could result in overfitting of the training data set[19;20] . Thus, multiple networks were created to ascertain the optimal number of neurons.

The architecture of the Neural Network Model, includ-

ing the various hyper-parameters, is summarized in Table 4. Figure 3 illustrates the neural network architecture, detailing the number of inputs, hidden layers, the number of neurons in each layer, and the output.

Table 4. Key parameters of the NN

Parameter
Hidden layers
Neurons in each layer
Optimizer
Activation function
Batch size
Epochs
Dropout

3.5 *Neural Network Architecture for Phase Fraction*

Similarly, the same Neural Network Architecture, the one developed for predicting the hardness values, was utilized for predicting the phase fractions of the steels, but instead of predicting hardness, Ferrite, Martensite, Pearlite, and Bainite microstructures were predicted. A distinct neural network, with a three-layer structure consisting of two hidden layers and an output layer, was established for each microstructure prediction. The strategy works because in a similar study by X Geng, X Mao, H.-H Wu, S Wang, W Xue, G Zhang, A Ullah, H Wang , develops hybrid machine-learning models to predict the phase transformation temperature and hardness of low alloy steel based on its chemical composition and cooling rate[21]

3.6 *Sensitivity analysis*

We conducted a sensitivity analysis to determine the impact of individual metal compositions on the hardness prediction of our model. For this, we employed a systematic approach where each metal composition was perturbed within a range of -5% to +5%, while all other variables were held constant. This method enabled us to assess the influence of each metal composition on the overall hardness prediction. We specifically focused on the absolute percentage change in predicted hardness as a response to changes in individual metal compositions. This approach elucidates how each composition affects hardness, providing insights into the critical factors for accurate hardness prediction.
It is crucial to note that this analysis relies on the assumption of independence between variables, which may only sometimes hold true in complex systems such as steel alloy composition. Additionally, the linearity of the response within the range of -5% to +5% variation may not be valid for larger perturbations. Despite these limitations, this analysis provides valuable preliminary insights into the model's sensitivity to changes in metal composition

4. Results

Table 5. R2Values Corresponding to the Number of Neurons

Number of Neurons in hidden layers	**Epochs**	**R^2 for testing data**	**R^2 for training and testing data**
[5,]	1000	0.895	0.889
[5, 5,]	1000	0.900	0.911
[10, 10,]	1000	0.958	0.963
[20, 20,]	1000	0.984	0.989

Table 6. ValuesCorresponding to the Number of Neurons

Phase Fractions	**R^2 for testing data**	**R^2 for training and testing data**
Ferrite	0.9855	0.9897
Martensite	0.9836	0.9906
Pearlite	0.9745	0.9931
Bainite	0.95552	0.98255

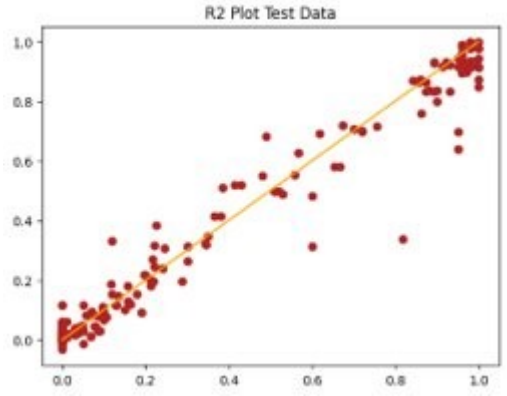

Figure 3.

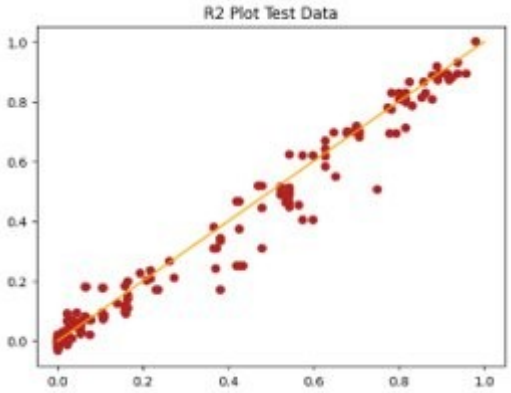

Figure 4.

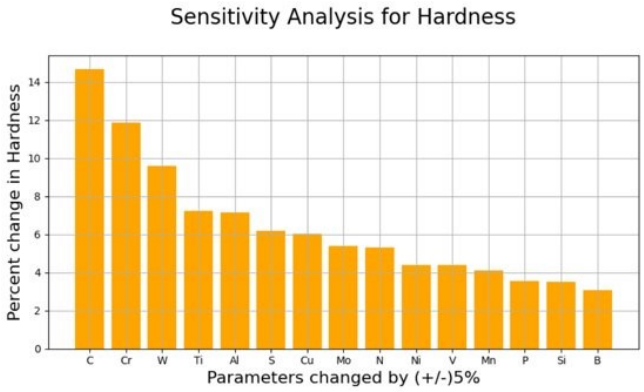

Graph 1: Senstivity Analysis

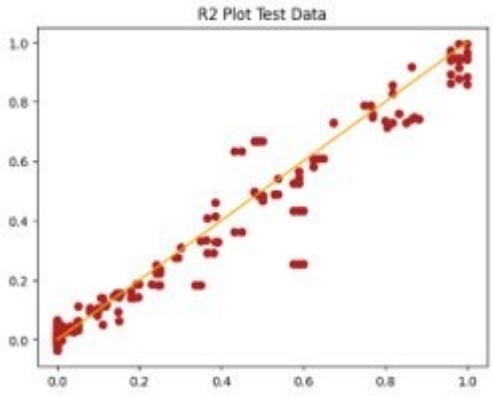

Figure 5.

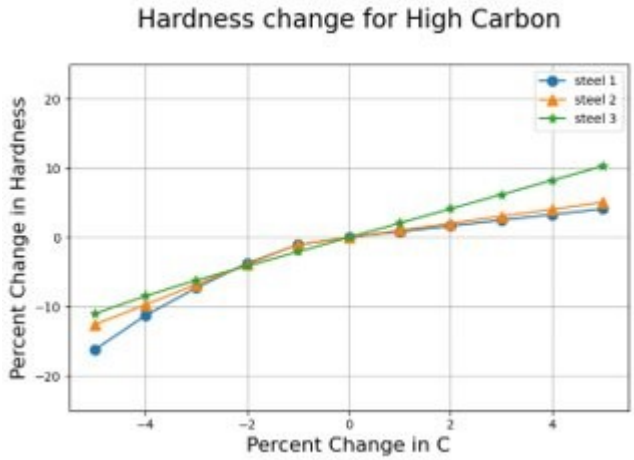

Graph 2: Trend in High Carbon Steel

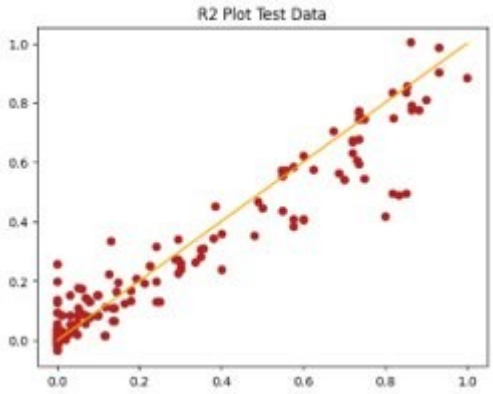

Figure 6.

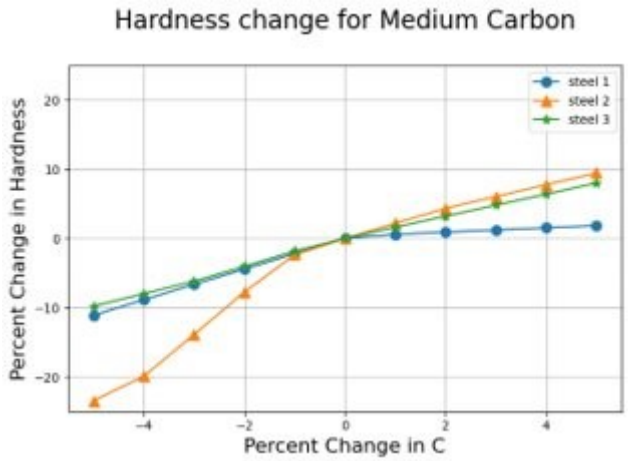

Graph 3: Trend in Medium Carbon Steel

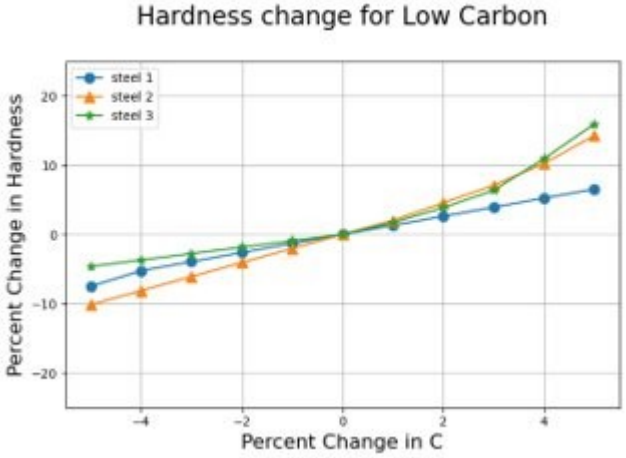

Graph 4: Trend in Low Carbon Steel

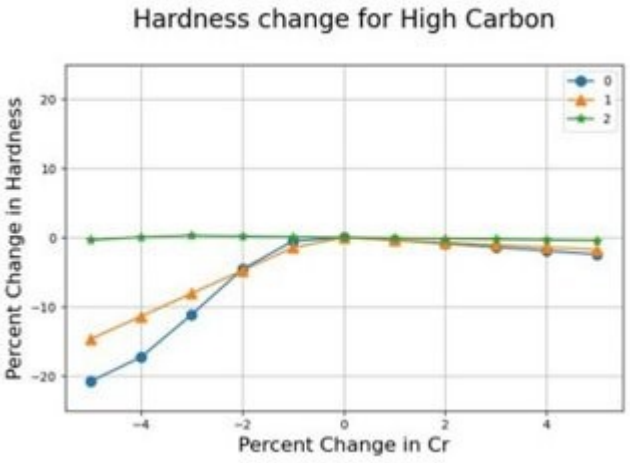

Figure 7.

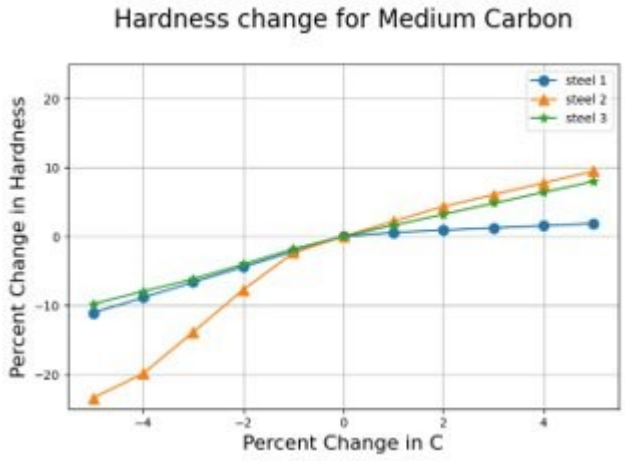

Figure 8.

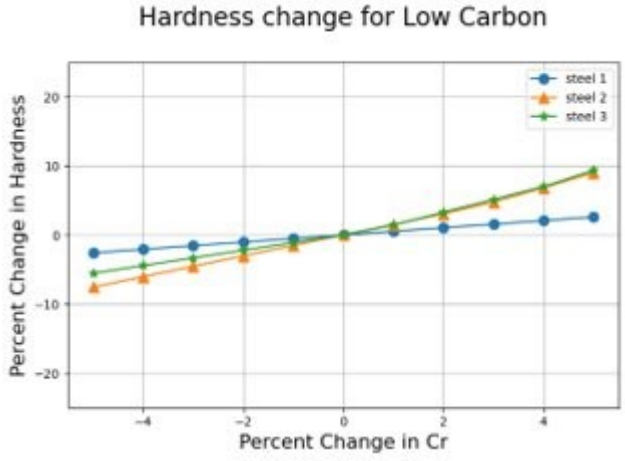

Figure 9.

5. Discussion

In this study, feed-forward neural networks were used to determine steel's harness and microstructure volume fractions. In the sensitivity analysis, we varied individual metal compositions by ±5% and observed the effect on predicted hardness.

5.1 *Neural Network Evaluation*

Several parameters were maintained consistently across all hyperparameter tuning exercises, as presented in Table 7 . These parameters yielded positive results when used in conjunction with various configurations of hidden layers, number of neurons, and epochs, and thus were not altered during the tuning process.

Table 7. Unchanged Parameters

Parameter	Value
Optimizer	Adam
Activation function	ReLu
Batch size	8
Dropout	0.1

TheTable 6 demonstrates that increasing the number of hidden layers and neurons when trained over a specified number of epochs, can significantly enhance the R-squared value.

A similar pattern was observed when calculating the R-squared value for phase fractions represented in table 7

5.2 *Sensitivity Analysis*

According to the Graph 1 carbon and chromium were identified as having the most significant impact on hardness, and futher analysis were done on both the elements.

5.2.1 *Analysis after altering only Carbon content* Graphs 2, 3 and 4 shows the trend of hardness increase with increase in carbon content.X Wang, Y Chen, S Wei, L Zuo, F Mao(2019) found that with increasing carbon content in the steels, the hardness increased and impact toughness decreased distinctly due to the increasing carbon supersaturation and refinement of martensite[22] . K Sotoodeh(2022) found that increasing the carbon content also increases the mechanical strength and hardness but decreases the ductility and weldability of carbon steel[23]. According to another study , the level of carbon content has an impact on both martensite hardness and hardenability. As the carbon content and martensite fraction increase, so do the hardness and strength[24].

5.2.2 *Analysis on after altering only Chromium content* P M Khanh, N D Nam, L T Chieu, H T N Quyen(2014) states that the hardness of high manganese steel increased when the chromium content increased, but the hardness was not much changing when the Cr contents changed from 2%

to 2.5% of the weight[25]. According to a paper published in Materials Science Forum, chromium tends to increase hardness penetration. This element has exciting effects on steel and improves the corrosion resistance of manganese steel. Chromium acts as a carbide former thus, excess of Cr to manganese steel will precipitate carbide at the grain boundary in the as-cast condition[26] .Y Tian, J Ju, H Fu, S Ma, J Lin, Y Lei(2019) shows that when the proper amount of chromium element was added, the micro-hardness of the matrix and macro-hardness of the alloy were relatively high. The hardness of the Fe-Cr-B alloy slightly decreased when the chromium content was more than 12 wt.%[27] .Similar behaviors are observed in Figures 7, 8 and 9 .

6. Conclusions

In conclusion, our study successfully developed a predictive model using a feed-forward neural network to determine hardness values and phase fraction percentages of steel during heat treatment under specific cooling conditions. The model demonstrated high accuracy, as assessed by the R^2 values obtained during the training and testing phases. Sensitivity analysis revealed that carbon and chromium were the key input variables with the most significant impact on hardness.

The findings of this research align with existing theoretical knowledge and experimental data, highlighting the effectiveness of the developed model in predicting steel properties under varied cooling conditions. The model incorporated input variables such as time and temperature pairs from cooling profiles and the chemical composition of the steel. The accurate prediction of phase fraction could guide us toward the optimal time-temperature cooling rate for steel production. By determining this optimum, we can tailor the manufacturing process to achieve the desired mechanical properties of steel. Not only does this enhance the quality and performance of the resulting product, but it also presents the potential for considerable cost reductions in the manufacturing process.

Overall, this study contributes to the understanding of the relationships between steel composition, heat treatment processes, and resulting properties. The developed predictive model can be a valuable tool for steel manufacturers and researchers, enabling more informed decision-making and the ability to tailor steel properties for specific applications.

References

[1] Celada-Casero, C, Huang, B M, Yang, J. R, and San-Martin, D. 2019. *Materials & Design*, **181** 107922–107922.

[2] Wang, S, Yu, G, Yang, W, Wang, Z, Jacobson, O, Tian, R, Deng, H, Lin, L, and Chen, X. 2021. *Advanced Science*, **8**.

[3] Shi, B L, Zhang, C, Tang, Y W, Wei, G J, Li, Y, He, C, and Xu, K. 2020. *Materials Science Forum*, **993** 575–584.

[4] Jung, I D, Shin, D S, Kim, D, Lee, J, Lee, M S, Son, H J, Reddy, N S, Kim, M, Moon, S K, Kim, K T, Yu, J. H, Kim, S, Park, S J, and Sung, H. 2020. *Materialia*, **11** 100699–100699.

[5] Bok, H. H, Kim, S N, Suh, D W, Barlat, F, and Lee, M. G. 2015. *Materials Science and Engineering: A*, **626** 67–73.

[6] Bohemen, S M C Van. 2018. *Materials Science and Engineering: A*, **731** 119–123.

[7] Huang, C. C, Chen, Y. T, Chen, Y. J, Chang, C. Y, Huang, H. C, and Hwang, R. C. 2009. *Fourth International Conference on Innovative Computing, Information and Control (ICICIC)*, pages 1216–1219.

[8] Monajati, H, Asefi, D, Parsapour, A, Abbasi, and Sh. 2010. *Computational Materials Science*, **49** 876–881.

[9] Sterjovski, Z, Nolan, D, Carpenter, K R, Dunne, D P, and Norrish, J. 2005. *Journal of Materials Processing Technology*, **170** 536–544.

[10] Sidhu, G, Bhole, S D, Chen, D L, and Essadiqi, E. 2011. *Computational Materials Science*, **50** 3377–3384.

[11] Sidhu, G, Bhole, S D, Chen, D L, and Essadiqi, E. 2012. *Materials & Design*, **41** 99–107.

[12] George, F, Vander, and Voort.

[13] Srinivasan, S. 2020. *ICTEA: International Conference on Thermal Engineering*, **2020**.

[14] Huang, X, Wang, H, Xue, W, Xiang, S, Huang, H, Meng, L, Ma, G, Ullah, A, and Zhang, G. 2020. *Computational Materials Science*, **171** 109282–109282.

[15] Geng, X, Wang, H, Xue, W, Xiang, S, Huang, H, Meng, L, and Ma, G. 2020. *Computational Materials Science*, **171**.

[16] & Zein, Hossam, Tran, & Abdelmotaleb, Vu, and Ghazy. 2015. How to Extract Data from Graphs using Plot Digitizer or Getdata Graph Digitizer.

[17] Farmer, J. 2018. *Australian Senior Mathematics Journal*, **32** 8–12.

[18] Pallavi, Joshi, Singh, S, Kaur, D, Lee, M, and N, H. 2022. *Archives of Computational Methods in Engineering*, **29** 4027–4047.

[19] Bhadeshia, H K D H, Dimitriu, R C, Forsik, S, Pak, J H, and Ryu, J H. 2009. *Materials Science and Technology*, **25** 504–510.

[20] Rojas, R. 1996. Neural Networks. Springer, Berlin Heidelberg.

[21] Geng, X, Mao, X, Wu, H. H, Wang, S, Xue, W, Zhang, G, Ullah, A, and Wang, H. 2022. *Journal of Materials Science & Technology*, **107** 207–215.

[22] Wang, X, Chen, Y, Wei, S, Zuo, L, and Mao, F. 2019. *Frontiers in Materials*.

[23] Sotoodeh, K. 2022. *Cryogenic Valves for Liquefied Natural Gas Plants*, pages 175–211.

[24] Concepción, V L De La, Lorusso, H N, and Svoboda, H G. 2015. *Procedia Materials Science*, **8** 1047–1056.

[25] Khanh, P M, Nam, N D, Chieu, L T, and Quyen, H T N. 2014. *Materials Science Forum*, **804** 297–300.

[26] Mahlami, C. S. and Pan, Xiaowei. 01 2014. *71st World Foundry Congress: Advanced Sustainable Foundry, WFC 2014*.

[27] Tian, Y, Ju, J, Fu, H, Ma, S, Lin, J, and Lei, Y. 2019. *Journal of Materials Engineering and Performance*, **28** 6428–6437.